

momentum $j = \frac{1}{2}$. (We could write, for example, $\mathbf{J} = \frac{1}{2}\boldsymbol{\sigma}$.) Substituting in (41) again, we get

$$D \rightarrow \frac{1}{3}(A+2B)k^2 + (e/6mc)(2Km-1)\mathbf{J}\cdot\mathbf{H} \\ = \frac{1}{3}(A+2B)k^2 + (e/12mc)(2Km-1)\boldsymbol{\sigma}\cdot\mathbf{H}. \quad (\text{b.9})$$

If we leave off the $\mathbf{J}\cdot\mathbf{H}$ term and choose the representation (39) for \mathbf{J} [in (b.7)], then (b.7) and (b.9) agree exactly with (V.13) of LK. It is easily seen by the methods of Sec. I that the form of (b.9) is the most general possible for the twofold degenerate case.

Experimental Cross Sections for Charge-Changing Collisions of He^+ and He^{++} Ions Traversing Gases*

S. K. ALLISON, J. CUEVAS,† AND P. G. MURPHY

The Enrico Fermi Institute for Nuclear Studies, University of Chicago, Chicago, Illinois

(Received February 6, 1956)

Ion beams of He^+ and He^{++} , in the kinetic energy range 100 to 450 kev, are held in arcs of circular orbits in a magnetic field. When a few microns of gas are admitted the beam is attenuated by charge-changing collisions, since with change of charge the ion is lost from its orbit. Cross sections for such charge-changing collisions are designated by σ_{if} , where i is the initial positive ionic charge in electron units and f the charge after the collision. ($\sigma_{10} + \sigma_{12}$) has been directly measured for He^+ in hydrogen, helium, and air, and ($\sigma_{21} + \sigma_{20}$) for He^{++} in the same gases.

Other observers have measured the equilibrium ratio $\text{He}^+/\text{He}^{++}$ attained in a field-free beam after many collisions, and combining these data with our observations allows calculation of σ_{10} and σ_{12} separately if one assumes σ_{02} negligible compared to the other cross sections. The electron loss cross sections σ_{12} increase with

energy for helium and air throughout the measured region and are of the order 10^{-17} cm²; σ_{12} for hydrogen vs energy shows a broad maximum at about 370 kev and 0.98×10^{-17} cm² per hydrogen atom.

The capture cross sections σ_{10} decrease rapidly in the measured energy range and in the region 200–450 kev those measured in helium agree, within the estimated experimental error, with theoretical calculations of H. Schiff.

In attempting the resolution of the sums ($\sigma_{21} + \sigma_{20}$) into the separate cross sections it is found that the errors in the measurements accumulate to such an extent that the individual values become very unreliable. An auxiliary experiment designed to increase the accuracy of our knowledge of the separated capture cross sections σ_{20} and σ_{21} is in progress.

1. INTRODUCTION

THE discovery by Henderson,¹ in 1922, that an appreciable fraction of the alpha particles emitted from natural sources have an orbital electron attached, and thus are He^+ ions, initiated a series of researches in which the capture and loss of electrons by moving helium ions were studied. The results on α particles prior to 1933 have been summarized in the *Handbuch der Physik* by Geiger,² and the same volume contains a review of work on the more general aspects of charge changing collisions, by R uchardt.³

The status of the problem as of June, 1953, has been recorded by Allison and Warshaw.⁴

Experimental researches on this problem may be roughly divided into two categories: (A) studies of the equilibrium ratios of the various charge states attained after a sufficiently large number of charge-changing collisions; (B) studies of the collision cross sections for individual charge-changing events.

Subsequent to the work summarized by Allison and Warshaw other reports of researches on helium ions under a category (A) have appeared from the Cavendish Laboratory⁵ and the Oak Ridge National Laboratory.⁶ Specific applications to the production of He^{++} beams for acceleration to high energies are reported by Bittner⁷ and by Geller and Prevot.⁸

The experimental studies reported here belong in category (B), and are in the kinetic energy range 100 to 450 kev. We shall use the notation σ_{if} in discussing the cross sections, where subscript i refers to the initial positive charge on the ion in units of the magnitude of the electronic charge, and f to the positive charge after the collisions in the same units. Very little was known of the helium cross sections in the range 100 to 600 kev when the summary by Allison and Warshaw was written. Some helium cross sections in the kinetic energy range up to 100 kev had been reported,^{9–14} and

* This work was supported in part by a grant from the U. S. Atomic Energy Commission.

† Now at Junta de Energia Nuclear, Madrid, Spain.

¹ G. H. Henderson, Proc. Roy. Soc. (London) **A102**, 496 (1922).

² H. Geiger, *Handbuch der Physik* (Verlag Julius Springer, Berlin, 1933), Vol. 22, Part 2, p. 221.

³ E. R uchardt, *Handbuch der Physik* (Verlag Julius Springer, Berlin, 1933), Vol. 22, Part 2, p. 103.

⁴ S. K. Allison and S. D. Warshaw, Revs. Modern Phys. **25**, 779 (1953).

⁵ G. A. Dissanaik, Phil. Mag. Ser. 7, **44**, 1051 (1953).

⁶ Stier, Barnett, and Evans, Phys. Rev. **96**, 973 (1954).

⁷ J. W. Bittner, Rev. Sci. Instr. **25**, 1058 (1954).

⁸ R. Geller and F. Prevot, Compt. rend. **238**, 1578 (1954).

⁹ P. Rudnick, Phys. Rev. **38**, 1342 (1931).

¹⁰ H. Meyer, Ann. Physik **30**, 635 (1937).

¹¹ F. Wolf, Ann. Physik **30**, 313 (1937), and previous publications.

¹² A. Rostagni, Nuovo cimento **15**, 117 (1939).

¹³ R. A. Smith, Proc. Cambridge Phil. Soc. **30**, 514 (1934).

¹⁴ J. P. Keene, Phil. Mag. Ser. 7, **40**, 369 (1949).

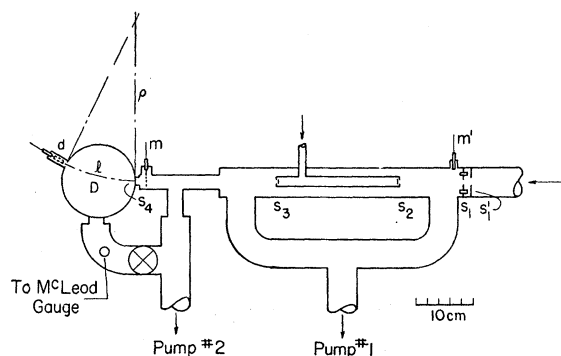


FIG. 1. Essential parts of the apparatus.

there are more recent results in this region by Stedeford and Hasted,¹⁵ and by Fedorenko.¹⁶ Krasner¹⁷ has reported cross sections σ_{01} in hydrogen, helium, and air using essentially the same equipment as that with which the present results were obtained, and Barnett and Stier¹⁸ have presented results for σ_{01} in the region from 30 to 200 kev.

2. EXPERIMENTAL METHOD

The experiments reported here are direct measurements of the cross-section sums $(\sigma_{10} + \sigma_{12})$ and $(\sigma_{21} + \sigma_{20})$ for helium beams traversing hydrogen, helium, and air respectively. The method is the second (ii) of those described on page 810 of the article by Allison and Warshaw.⁴

For the measurement of $(\sigma_{10} + \sigma_{12})$ a beam of He^+ ions is held in a circular orbit as it traverses a measuring cell, by placing the cell between the poles of a powerful electromagnet. With the gas pressure in the cell so low that the mean free paths for all possible collision types are much longer than the cell dimensions, one measures the flux of ions leaving the cell through an aperture whose dimensions are small compared to the displacement of the emergent beam caused by the magnetic field. The introduction of gas attenuates this beam due to charge changing collisions which cause the ion to be lost from its orbit. If the length of path along the arc through the gas is known, and the pressure is measured,

$$\sum \sigma_{ij} = \frac{kT}{Pl\xi} \ln \frac{R(0)}{R(p)}, \quad (1)$$

where $\sum \sigma_{ij}$ is the total cross section per atom of gas traversed for all processes which may change the ion orbit, k is Boltzmann's constant, 1.380×10^{-16} erg/°K, T is the temperature of the gas in the measuring cell in °K, P is the pressure in dynes/cm² in the measuring cell which corresponds to the attenuated flux $R(p)$, l is

the effective beam length along the curved path in the measuring cell, ξ is the number of atoms per molecule of gas. $R(0)$ is a measured quantity proportional to the unattenuated flux of ions emerging from the cell, and $R(p)$ is proportional to the attenuated flux when gas is added.

The ion beams used in the experiment were supplied by a Cockcroft-Walton accelerator, or kevatron, which had a standard type of radio-frequency ion source¹⁹ and produced a beam of 10–30 microamperes of He^+ at energies from 100 to 450 kev. The accelerated ion beam from the kevatron, which contained some H^+ even after long operation on Government Grade A helium, was angularly dispersed into a momentum spectrum by the kevatron magnet, and the He^+ constituent was deviated $22\frac{1}{2}^\circ$ from the kevatron accelerator tube axis into the chambers used for this experiment. For studies of $(\sigma_{10} + \sigma_{12})$, the He^+ beam as it came from the kevatron could be used without modification, but He^{++} had to be obtained by charge equilibration of the He^+ beam in an "equilibration chamber" which preceded the measuring chamber in which the cross sections were determined. The apparatus was essentially that of Fig. 1 of Krasner's paper, with some modifications described below. A schematic diagram is given here as Fig. 1 of this report. Some pertinent dimensions are given in Table I.

In Fig. 1, the insulated disk at s_1 is connected to a galvanometer through lead m' . This serves as an indicator to assist in directing the He^+ beam along the axis of the system. In order to monitor the equilibrated beam before it enters the measuring chamber, part of it is intercepted on a fine mesh grid at m . For reliable monitoring by such a screen its mesh must be fine compared to the cross-section area of the beam. The screen selected is commercially available²⁰ and has 200 openings to the inch. The openings are square, and 0.002 inch on a side; the transmission is 16%, and the thickness is 0.002 inch. Thus there are approximately 250 apertures in this screen across the beam which is circular and 0.0914 cm in diameter. The current intercepted by this screen was allowed to charge up a high quality condenser and was integrated by observing the rise of voltage on a suitable electrometer.

The detector d was of the type first described by

TABLE I. Data concerning apparatus (see Fig. 1).

s_1'	0.318 cm diam	
s_1	0.226 cm diam	
s_2	0.0914 cm diam	$s_1 - s_2 = 12$ cm
s_3	0.0914 cm diam	$s_2 - s_3 = 20.63$ cm
s_4	0.199 cm diam	$s_1 - s_4 = 61$ cm
D	12.70 cm	slit at d , 0.41 cm wide;
l	12.40 cm	in some runs; 0.278 cm wide.

¹⁵ J. B. H. Stedeford and J. B. Hasted, Proc. Roy. Soc. (London) **A227**, 466 (1955).

¹⁶ N. V. Fedorenko, Zhur. Tekh. Fiz. **24**, 769 (1954).

¹⁷ S. Krasner, Phys. Rev. **99**, 520 (1955).

¹⁸ C. F. Barnett and P. M. Stier, Phys. Rev. **100**, 1268(A) (1955).

¹⁹ Adapted from the design of Moak, Reese, and Good, Nucl. Electronics **9**, 18 (1951).

²⁰ "Lektromesh" screen from C. O. Jelliff Manufacturing Corporation, Southport, Connecticut.

Montague,²¹ in which the ion beam impinged on a beryllium-copper plate biased negative with respect to the detector housing, and the primary ion current is amplified by the emission of secondary electrons.

The tubes of Fig. 1 through which the ion beam passed were built of mild steel, in order to shield the beam from the stray field of the magnet between the poles of which the measuring chamber was placed.

All pressure measurements used in computing cross sections were made on a sensitive McCleod gauge (311.7 cc bulb, 0.0803 cm radius capillary).

3. METHOD OF MEASUREMENT

The kevatron was adjusted to the desired voltage, and the ion beam from the radio-frequency ion source operating on helium gas was focused. By means of the sorting magnet of the kevatron, the He^+ constituent was directed down the axis of the measuring system, (Fig. 1).

If measurement of a cross section for He^{++} ions was desired, a convenient pressure (5–15 microns) of gas was introduced into the equilibration cell (between s_2 and s_3), using the same gas which would later be used in the measuring chamber for the cross-section determinations. For He^+ measurements, no gas was needed in the equilibration cell, in fact, many of the measurements on He^+ were taken without the interposition of the equilibration cell into the beam.

The magnetic field on the measuring chamber was then adjusted until the desired ionic component (He^{++} or He^+) was directed into the detector at d .

The rate of rise of potential of a condenser, charged by the fraction of the equilibrated beam intercepted at m , was noted on a quadrant electrometer, and by means of a multiple throw switch a capacity was selected which would result in a suitable deflection in about 30 seconds.

A similar selection of a suitable capacity in the detector circuit, in which the measuring device was a vibrating reed electrometer, was made so that a convenient deflection resulted in the same time interval. A beam flux measurement consisted in measuring the potential acquired by the detector condenser when the monitor condenser had reached a predetermined charge, thus integrating both currents.

When measurements were under way on He^{++} , the presence, in the measuring chamber, of the considerably more intense He^+ beam caused some difficulty. When the magnetic field was so adjusted that the He^{++} beam was deflected 30° and therefore passed into the detector at d , the He^+ beam was deflected 15° toward d from the undeviated position. When gas was admitted for an attenuation measurement on He^{++} , there was electron loss from this He^+ beam, and a "spray" of new He^{++} ions fanned out from it toward larger angles of deviation, producing a background under the at-

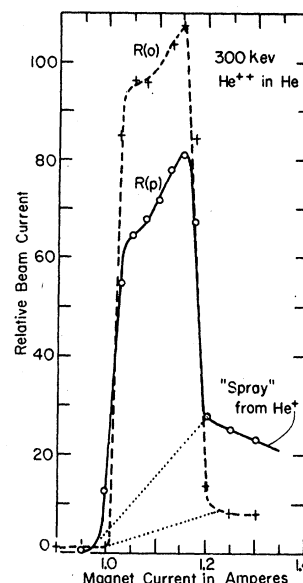


FIG. 2. Attenuation of a 300-kev He^{++} beam in helium gas through charge changing collisions in a magnetic field. The magnetic field, about 3300 gauss, produces 30° deviation of the beam when acting on 12.40 cm of path.

tenuated He^{++} beam. This was revealed, see Fig. 2, by increasing the magnetic field slightly so that the attenuated He^{++} beam no longer entered the detector slit, and the background under it was exposed.

After several methods had been thought up and tested for correcting the attenuated He^{++} intensity for this effect, the most certain, but most tedious, of them was adopted. This consisted in running a complete profile of both the "gas out" and attenuated beams, sweeping them across the detector slit by varying the magnetic field and taking care to measure the level of the background on the high and low magnet side of the peak. A set of data is shown in Fig. 2, which is a measurement of $(\sigma_{21} + \sigma_{20})$ for 300-kev He^{++} ion in helium gas. The "gas out" pressure was 0.70 micron of mercury (rather higher than usual) and although the relevant σ_{12} cross section is rather small ($1.2 \times 10^{-17} \text{ cm}^2$), the 11.2 times higher intensity of the He^+ beam causes an appreciable He^{++} spray even with gas out. When 8.62 microns of helium was admitted, to produce the attenuated curve of Fig. 2, we see that the spray has greatly increased. There is no spray on the low magnet current side of the peak because no He^{++} ions formed anywhere along the He^+ beam can enter the slit if the magnetic field is too weak to deviate the true He^{++} beam sufficiently. Since the width of the slit in the direction of the sweep of the beam was 0.41 cm and the effective diameter of the beam at the detector aperture was 0.188 cm,²² the profile should have a flat top. However, the shape of the peaks at the top indicates that they are superimposed on a sloping background. The dotted lines under the peaks of Fig. 2 show how much was subtracted from the area for this "spray effect." The areas between the reconstructed backgrounds and the profiles were measured by cutting out the curves and weighing them. Making

²¹ J. Montague, Phys. Rev. **81**, 1026 (1950).

²² S. Krasner, reference 17, p. 523.

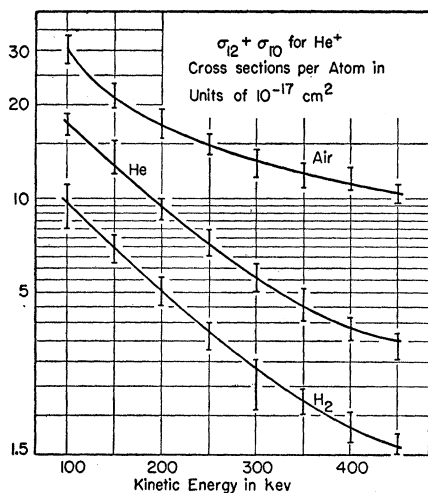


FIG. 3. Cross sections from experiments on the attenuation of a He^+ beam when ions which have changed their charge are removed.

the spray correction in this manner corresponded to using the full path length of 12.40 cm as the effective length l .

In the example of Fig. 2, the ratio of areas, or the fractional attenuation, $R(p)/R(0)$, was 0.637. The temperature of the measuring cell was 20°C , and with $l=12.40$ and $\xi=1$, the coefficient of the logarithm in Eq. (1) is 3.51×10^{15} . The resultant $(\sigma_{20} + \sigma_{21})$ is $13 \times 10^{-17} \text{ cm}^2$ per helium atom.

When low cross sections are measured, such as $(\sigma_{10} + \sigma_{12})$ for 400 keV He^+ in hydrogen, where the value is $0.9 \times 10^{-17} \text{ cm}^2$, relatively large amounts of hydrogen must be let into the measuring cell to produce sufficient attenuation for accurate measurement. In our measurements 21.0 microns were admitted. It was thought advisable to test again²³ whether the detector was "gas sensitive." This was done by directing the 400-keV proton beam from the kevatron, always present even when operating on helium, into the measuring cell, and then deviating it into the detector. At 400 keV the capture cross section σ_{10} for protons is so small that the beam remains 100% charged, so that no attenuation

TABLE II. $(\sigma_{10} + \sigma_{12})$ in units of 10^{-17} cm^2 per gas atom.

Helium ion kinetic energy (keV)	Hydrogen		Helium		Air	
	Best	Uncertainty	Best	Uncertainty	Best	Uncertainty
100	9.8	± 2.0	17.5	± 1.0	30	± 3
150	7.0	± 0.7	13.0	$+3.0, -1.0$	21.6	± 2.2
200	5.1	± 0.5	9.5	$+0.5, -1.5$	17.5	± 1.8
250	3.8	$+0.2, -0.7$	7.2	± 0.7	15.0	± 1.5
300	2.8	$+0.3, -0.7$	5.6	± 0.6	13.4	± 1.3
350	2.2	± 0.2	4.6	± 0.5	12.3	± 1.2
400	1.9	± 0.2	3.9	± 0.4	11.5	$+1.7, -0.7$
450	1.5	± 0.2	3.4	± 0.3	10.6	± 1.1

²³ J. Montague, reference 21, p. 1031.

was to be expected. When 21 microns of H_2 was admitted, the detector response to the proton beam actually increased, as Montague had previously found, and by about 6%. This is presumably due to ionization of the gas in the detector cavity by the ion beam and the secondary electrons. The magnitude of the effect is roughly the same as in Montague's work, and an appropriate correction was made to our measurements.

4. EXPERIMENTAL RESULTS

The direct experimental results of the series of measurements reported here are the cross-section sums $(\sigma_{10} + \sigma_{12})$ and $(\sigma_{21} + \sigma_{20})$. The results are displayed in graphical form in Figs. 3 and 4, and tabulated in Tables II and III. Estimates of the uncertainties in the values are included. As previously experienced in

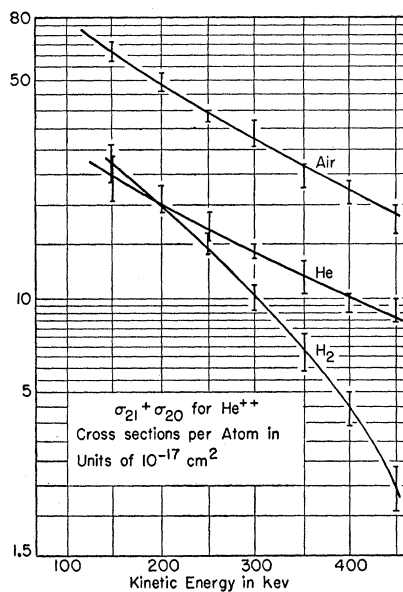


FIG. 4. Cross sections from experiments on the attenuation of a He^{++} beam when ions which have changed their charge are removed.

taking this type of measurement, it was found more difficult to reproduce results in the lighter gases, especially hydrogen, than in air. We do not have an explanation of this; one guess is that the reducing action of ionized hydrogen gas affects the secondary electron yield from our detectors by acting on their surfaces.

In certain cases we have recommended a "best" value which does not lie centrally in the region of uncertainty. This choice has, of course, been influenced by neighboring points on the curve, and by the presumption that the choice producing the minimum change in slope and curvature is the best choice, a sort of primitive least squares method.

5. CALCULATION OF INDIVIDUAL CROSS SECTIONS

If the results expressed in Tables II and III are combined with other results concerning the charged

TABLE III. ($\sigma_{20} + \sigma_{21}$) in units of 10^{-17} cm².

Helium ion kinetic energy (keV)	Hydrogen		Helium		Air	
	Best	Uncertainty	Best	Uncertainty	Best	Uncertainty
100	(38) ^a	+0.0, -6.0	(28) ^a	±4.0	(79) ^a	±8.0
150	27.5	±3.0	24.5	±4.0	62	±5.0
200	20.0	+3.0, -1.0	20.0	+3.0, -1.0	49.5	±3.0
250	14.5	+2.0, -1.0	16.6	+2.5, -1.0	40.0	+0.0, -2.5
300	10.1	±1.0	14.0	+1.0, -0.4	32.5	±2.0
350	7.0	±0.7	11.7	±1.2	26.8	+0.0, -3.0
400	4.5	+0.4, -0.6	10.0	+0.1, -1.0	22.2	±2.0
450	2.5	±0.3	8.6	+1.5, -0.1	18.2	±1.5

^a Values in parentheses were extrapolated beyond the region of taking data.

states of helium beams, it is possible to calculate individual cross sections from them. The necessary formulas can be developed from the treatment by Allison and Warshaw.⁴ Their equations (23'') are

$$\begin{aligned}\phi_0 &= [\sigma_{10}(\sigma_{21} + \sigma_{20}) + \sigma_{20}\sigma_{12}]/D, \\ \phi_1 &= [\sigma_{21}(\sigma_{02} + \sigma_{01}) + \sigma_{01}\sigma_{20}]/D, \\ \phi_2 &= [\sigma_{02}(\sigma_{10} + \sigma_{12}) + \sigma_{12}\sigma_{01}]/D,\end{aligned}\quad (2)$$

in which ϕ_i is the fraction of ions of positive charge i , in electron units, in the entire equilibrated beam, and

$$D = \sigma_{12}(\sigma_{01} + \sigma_{02} + \sigma_{20}) + \sigma_{10}(\sigma_{21} + \sigma_{02} + \sigma_{20}) + \sigma_{21}(\sigma_{01} + \sigma_{02}) + \sigma_{01}\sigma_{20}. \quad (3)$$

If we introduce the equilibrated ratio He⁺/He⁺⁺, and call it r_{12} , we obtain

$$r_{12} = \phi_1/\phi_2 = \frac{\sigma_{21}(\sigma_{02} + \sigma_{01}) + \sigma_{01}\sigma_{20}}{\sigma_{02}(\sigma_{10} + \sigma_{12}) + \sigma_{12}\sigma_{01}}. \quad (4)$$

TABLE IV. Equilibrium ratios He⁺/He⁺⁺ and He⁰/He⁺⁺ for helium beams in various gases. Sn≡E. Snitzer, Phys. Rev. **89**, 1237 (1953); St≡Stier, Barnett, and Evans, Phys. Rev. **96**, 973 (1954).

Kinetic energy (keV)	Hydrogen				Helium				Air			
	Sn	r_{12}	St	r_{02}	Sn	r_{12}	St	r_{02}	Sn	r_{12}	St	r_{02}
100	...	~300	...	~800	...	~50	...	~130	~100	~100	...	~150
150	~50	100	...	134	~50	38	43.5	58	~50	35	~15	31
200	31	...	18	36	22.8	25	16.0	27	23.7	18.1	8.66	9.9
250	21.7	...	8.2	...	16.5	...	8.93	...	13.1	...	3.47	...
300	12.5	...	3.17	...	11.2	...	4.67	...	8.0	...	1.58	...
350	7.03	...	1.35	...	7.72	...	2.45	...	5.25	...	0.893	...
400	4.62	...	0.62	...	5.93	...	1.42	...	3.74	...	0.500	...
450	3.38	...	0.39	...	4.41	...	0.84	...	2.74	...	0.260	...

TABLE V. Values of σ_{12} in units of 10^{-17} cm² per atom, computed by Eq. (5) from Tables III and IV.

Helium ion kinetic energy (keV)	γ_2^a	Hydrogen		Helium		Air	
		Best	Uncertainty	Best	Uncertainty	Best	Uncertainty
100	1.99	0.13 ^b	+0.01, -0.02	0.56 ^b	±0.1	0.79 ^b	±0.12
150	1.62	0.28 ^b	±0.03	0.64 ^b	±0.1	1.25	±0.16
200	1.40	0.64	+0.1, -0.03	0.88	+0.14, -0.04	2.09	±0.16
250	1.26	0.67	+0.09, -0.05	1.00	+0.16, -0.07	3.05	±0.18
300	1.15	0.81	±0.08	1.25	+0.09, -0.05	4.06	±0.32
350	1.06	1.00	±0.10	1.52	±0.11	5.10	±0.36
400	0.994	0.97	+0.08, -0.14	1.68	+0.03, -0.16	5.94	±0.40
450	0.937	0.74	±0.08	1.95	+0.37, -0.03	6.64	±0.44

^a γ_2 = (orbital velocity of electron in He⁺)/(translational velocity of He⁺ ion).

^b Values of r_{12} used to compute this cross section were taken from Stier, Barnett, and Evans, Phys. Rev. **96**, 973 (1954).

We will now make the assumption that σ_{02} is small compared to the other cross sections. This cross section concerns the ionization loss of both electrons from a moving helium atom in a single encounter. Classically it involves the product of the probability that one electron in the helium atom passes near enough to the effective positive core of a gas atom to receive more than 24.5 electron volts energy, while, simultaneously, the second is near enough to receive more than 54 electron volts. With this approximation, Eq. (4) becomes

$$r_{12} = (\sigma_{21} + \sigma_{20})/\sigma_{12},$$

or

$$\sigma_{12} = (\sigma_{21} + \sigma_{20})/r_{12}. \quad (5)$$

Thus, measured values of r_{12} , shown in Table IV, when combined with values of $(\sigma_{21} + \sigma_{20})$ from Table III, should, if our assumption is valid, permit calculation of σ_{12} ; then σ_{10} can be obtained, by subtraction, from the values in Table II.

The values of σ_{12} which result from Eq. (5), and the values in Tables III and IV, are shown in Table V. In compiling the best, or recommended values, the equilibrium ratio data of Stier, Evans, and Barnett⁶ have been used in certain cases, notably where Snitzer⁴ gave no equilibrium ratios, and in certain cases where the results of Stier *et al.* seem to lead to a smoother curve of σ_{12} vs energy.

Values of σ_{10} may be obtained by subtracting the σ_{12} values from the measured total cross section of Table II. The results are shown in Table VI.

It is formally possible to proceed to the calculation of σ_{21} , since from the relations of Eqs. (2), plus the assump-

TABLE VI. Values of σ_{10} in units of 10^{-17} cm² per atom of gas traversed. Computed by subtraction of Table V from Table II.

Helium ion kinetic energy (kev)	Hydrogen		Helium		Air	
	Best	Uncertainty	Best	Uncertainty	Best	Uncertainty
100	9.7	±2.0	16.9	±1.0	29	±3.0
150	6.7	±0.7	12.4	+3, -1	20.4	±2.2
200	4.5	±0.5	8.6	+0.5, -1.5	15.4	±1.8
250	3.1	+0.2, -0.7	6.2	±0.7	12.0	±1.5
300	2.0	+0.3, -0.7	4.4	±0.6	9.3	±1.6
350	1.2	±0.2	3.1	±0.5	7.3	±1.3
400	0.9	±0.2	2.2	+0.6, -0.4	5.6	±1.3
450	0.8	±0.3	1.5	+0.3, -0.7	4.0	±1.0

tion that σ_{02} is negligible, we obtain

$$\sigma_{21} = (\sigma_{10} + \sigma_{12})r_{12} - \sigma_{01}r_{02}. \quad (6)$$

However, in the lower part of our energy range, up to 300 kev, He^{++} is a very minor constituent of the equilibrated beam (<13%), and its change into He^+ or He^0 offers a negligible contribution to either of these dominant beam constituents. Thus the observed equilibrium ratios are insensitive to the partition of the total ($\sigma_{21} + \sigma_{20}$) into σ_{20} and σ_{21} and accurate values cannot be obtained.

In the upper part of the energy range the equilibrium fraction of He^0 is small and there are relatively large errors in its measurement. Thus calculated values of σ_{21} , using Krasner's data¹⁷ for σ_{01} , which are included in Figs. 5, 6, and 7, fluctuate widely and are very inaccurate. Stier, Barnett, and Evans⁶ have assumed that both the double-loss cross section σ_{02} and the double-capture cross section σ_{20} are negligible with respect to the other single electron charge changes.

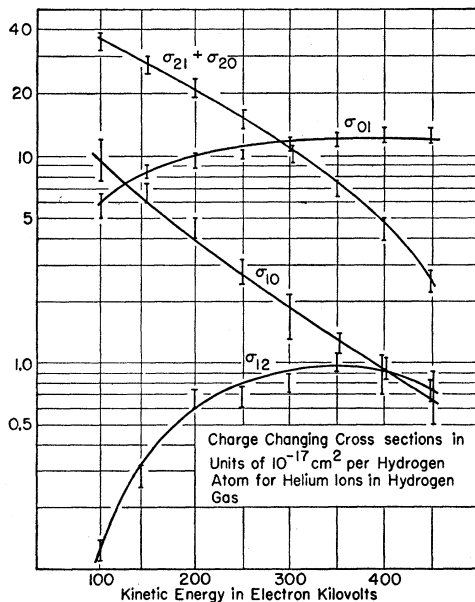


FIG. 5. Charge-changing cross sections for helium ions in hydrogen gas.

We are not yet ready to assume that σ_{20} is negligible; there appears to be some indication from Eq. (6) applied to our values that within a wide margin of error, such a double capture occurs in He^{++} ions of 300–400 kev kinetic energy passing through hydrogen gas.

An experiment intended to give greater precision in the estimates of the individual cross sections σ_{20} and σ_{21} is in progress in our laboratory. We hope to observe the initial ratios He^+/He^0 as a pure He^{++} beam is passed through the equilibration cell and the pressure increased in small steps above that in which the length of the cell is large compared to the mean free path for any charge changing collision. When this work is completed we expect to report the individual values σ_{21} and σ_{20} rather than their sums.

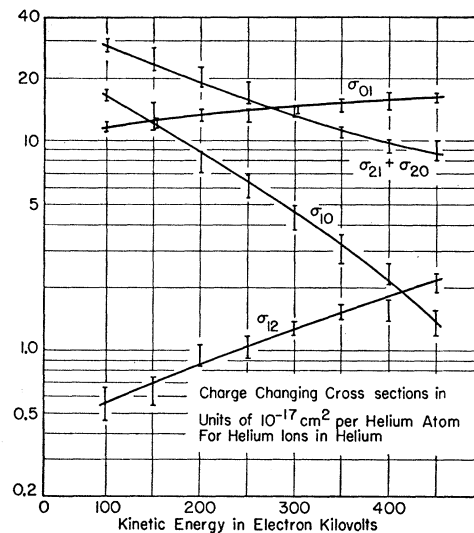


FIG. 6. Charge-changing cross sections for helium ions in helium gas.

6. DISCUSSION OF THE RESULTS

The cross section σ_{12} is an electron-loss cross section. Other loss cross sections which have now been studied in hydrogen and helium are $(\sigma_{01} + \sigma_{02})$ for moving helium atoms¹⁷ (which is presumably all σ_{01}) and σ_{01} for moving hydrogen atoms.²³ Let us define γ_i , introduced by Knipp and Teller,²⁴ by

$$\gamma_i = V_i/V, \quad (7)$$

where V_i is the orbital velocity of the most loosely bound electron in the moving ion, and V is the translational velocity. For a moving He^+ ion, V_2 is calculated from

$$V_2 = (2I_2/m)^{1/2}, \quad (8)$$

where I_2 is the second ionization potential of He^+ , or 54.14 volts. Values of γ_2 are given in Table V. In the

²⁴ J. Knipp and E. Teller, Phys. Rev. 59, 659 (1941).

case of σ_{12} for He⁺ passing through hydrogen, if we consider a system of coordinates in which the He⁺ is at rest, the removal of the electron from the He⁺ is accomplished by the energy transfer from moving protons, whose charge is partially screened by the electrons around them. Classically, the threshold for transferring the necessary 54.14 electron volts from a moving proton to an electron at rest occurs at a proton kinetic energy of 24.9 kev. In the laboratory system this corresponds to a helium ion kinetic energy of 99.5 kev. Making allowance for the motion of the electron in He⁺, we can at least anticipate a rapid rise in σ_{12} as the helium ion kinetic energy rises in the vicinity of 100 kev, and this appears on the hydrogen curve, Fig. 5. The maximum in σ_{12} in hydrogen occurs in the vicinity of $\gamma_2=1$, as anticipated from incomplete evidence in Krasner's paper. However, the cross section for strip-

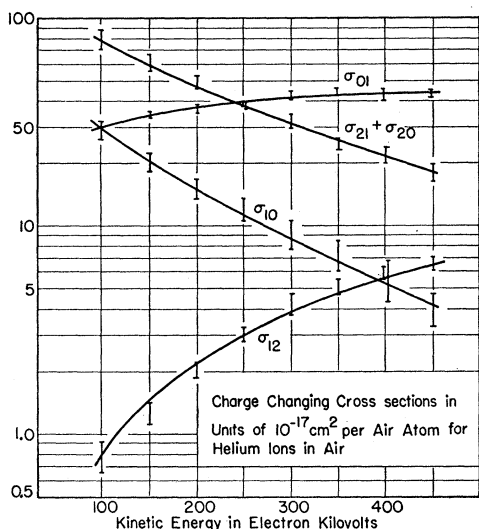


FIG. 7. Charge-changing cross sections for helium ions in air.

ping electrons from moving helium or hydrogen ions in hydrogen gas does not seem to be only a function of γ (see Krasner, Fig. 6). The cross sections σ_{12} at the same values of γ are much lower than $\frac{1}{2}\sigma_{01}$.

Barnett and Stier¹⁸ have reported some measurements of σ_{01} for helium ions in various gases, which in some cases are considerably lower than those of Krasner.¹⁷ They have suggested that in selecting the neutral component from an equilibrated beam, it is not certain that all the helium atoms in the beam are in the ground state (1s)²1S₀; there may be an appreciable fraction in the metastable state (1s2s)1S₀. The cross section for stripping an electron from the metastable state would presumably be greater, at the same velocity, than from the ground state. The fraction in the metastable state might possibly depend on the nature and pressure of the gas in which charge equilibration takes place.

We do not have any direct evidence as to what

TABLE VII. Conditions for $\phi_1=\phi_0$.

Gas traversed	Critical kinetic energy of moving ions (kev)	
	Estimated by Snitzer; see Table IV	Predicted by equality of σ_{01} and σ_{10} ; see Figs. 5, 6, 7
Hydrogen	148	130±20
Helium	145	150±15
Air	98	100, +10, -20

fraction, if any, of the neutral beam is in the metastable state under given conditions. However, there is some internal evidence in the experiments of our group that the neutral constituent of the equilibrated beam observed by Snitzer,⁴ had the same composition as the neutral beams whose cross sections σ_{01} were measured by Krasner¹⁷ and the same composition as those neutrals produced by the process σ_{10} in the present experiments. This comes from a consideration of those kinetic energies of motion at which the equilibrated beam shows equal fractions of He⁺ and He⁰. At the energies at which these equalities occur, He⁺⁺ is a negligible constituent of the equilibrated beam, and the postulated equality calls for equal values of σ_{01} and σ_{10} . Snitzer estimated the energies E_0 at which $\phi_1=\phi_0$, and we can compare them with the energies at which $\sigma_{01}=\sigma_{10}$ from Figs. 5, 6, and 7. This is shown in Table VII. The agreement is within the estimated errors.

Schiff²⁵ has made theoretical studies of certain capture cross sections for helium ions traversing gaseous hydrogen and helium. The methods of calculation were those of Jackson and Schiff,²⁶ in which they used the complete perturbation Hamiltonian, including the interaction of the two nuclei between themselves, in addition to their interactions with the electrons, and calculated by the Born approximation. This method, applied to the calculation of the capture of electrons by protons moving through hydrogen gas has given

TABLE VIII. Comparison of experimental and theoretical values of certain cross sections. Cross sections in cm² per atom of traversed gas, $\times 10^{17}$. σ_{21}' ~ capture into first excited state.

Kinetic energy of helium ions (kev)	σ_{10} for He ⁺ in helium gas			He ⁺⁺ in hydrogen gas		
	Experiment			$(\sigma_{21}+\sigma_{20})$		
	Snitzer ^a	This report	Theory Schiff ^b	Experiment, this report	Theory, Schiff ^b σ_{21}	σ_{21}'
100	...	16.9	30	(38)	180	70
131	17.2	...	20
150	...	12.4	17	27.5	80	32
200	...	8.6	10	20.0	44	16
250	...	6.2	6.3	14.5	23	8.2
300	...	4.4	4.5	10.1	15	4.8
340	3.1	...	3.2
350	...	3.1	3.0	7.0	8.3	3.0
400	...	2.2	2.2	4.5	5.2	2.0
450	...	1.5	1.8	2.5	3.5	1.3

^a See reference 6.
^b See reference 25.

²⁵ H. Schiff, Can. J. Phys. 32, 393 (1954).

²⁶ J. D. Jackson and H. Schiff, Phys. Rev. 89, 359 (1953).

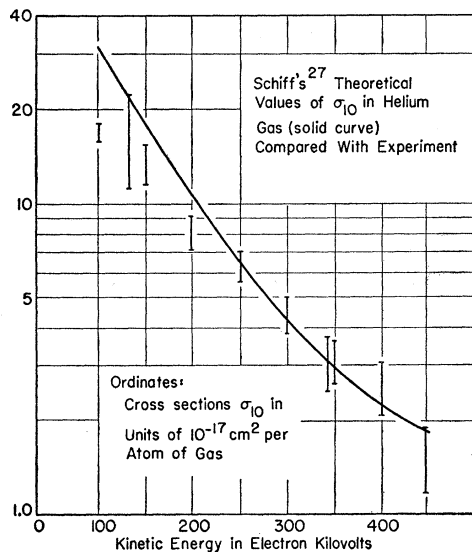


FIG. 8. Comparison of theoretical calculations on the capture of electrons by He^+ ions moving in helium gas with experiment.

surprisingly close agreement with the measurements in the 25- to 150-keV region.

Schiff has calculated the cross section σ_{10} for He^+ ions moving in helium gas, and between 200 and 400 keV kinetic energy there is remarkable agreement with our measured values, including some rough estimates of σ_{10} made by Snitzer during his experiments. The extent of the agreement is shown in Table VIII and Fig. 8.

Schiff has also calculated σ_{21} , the cross section for single electron capture by He^{++} moving in hydrogen gas, and has given values for the capture cross section into the first excited state, as well as the sum of the capture probabilities into the excited states plus the ground state. The experimental method used here does not distinguish between capture into excited states and capture into the ground state, and only measures their sum, since any capture which changes the ion orbit is counted.

Our opinion is that the experimental situation at present does not warrant a breakdown of the sum

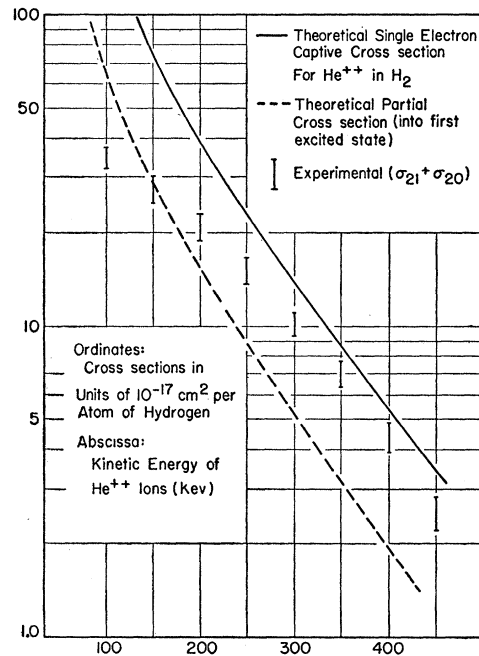


FIG. 9. Comparison of theoretical calculations of single electron capture by He^{++} ions in hydrogen with the measured cross-section sum ($\sigma_{20} + \sigma_{21}$). The experiment does not distinguish capture into the ground state from capture into an excited state.

$\sigma_{20} + \sigma_{21}$ into the separated cross sections. Thus the experimental sum can only serve as indicating an experimental maximum for σ_{21} .

A comparison is made in Table VIII and Fig. 9. It is seen that there is lack of agreement in the range 100–200 keV, and that between 200 and 450 keV the theoretical result is of the order of 50% greater than the maximum consistent with our experiments.

ACKNOWLEDGMENTS

We wish to thank Margarita Cuevas for much assistance in taking data and computing results, and John Erwood for helping to construct and maintain the equipment used.